STRUCTURE AND DYNAMICS OF THE 60-140 KM REGION ON MARS. T. L. McDunn[1] and S. W. Bougher[2], J. Murphy[3], M. D. Smith[4], F. Forget[5], J.-L. Bertaux[6], F. Montmessin[7], [1]University of Michigan (2455 Hayward St., Ann Arbor, MI 48109, tmcdunn@umich.edu), [2]U. of Michigan (2455 Hayward Avenue, Ann Arbor, MI 48109, bougher@umich.edu), [3]New Mexico State University, [4]NASA GSFC, [5]Laboratoire de Météorologie Dynamique, [6]Service D'Aéronomie, [7]Service D'Aéronomie.

Introduction: The Martian middle atmosphere (~60-140 km) is notoriously understudied, yet important for several reasons. It is the region across which the lower and upper atmosphere are coupled and information is passed from the lower atmosphere to the solar UV- and EUV-dominated upper atmosphere. As a result, it experiences mechanisms and phenomena that are unique to these altitudes, and which must be understood in order to develop a full understanding of the dynamical coupling between the lower and upper atmospheres. In addition, this altitude range is of large import for aerobraking and aerocapture missions. An additional motivation for this study is that appropriate lower boundary conditions are essential in order to accurately simulate the interaction between the solar wind and the Martian upper atmosphere. Such boundary conditions are provided by thermospheric general circulation models such as the coupled multi-dimensional MGCM-MTGCM.

Since the mid-1990's there has been a significant increase in the number of datasets available for the Martian atmosphere. Our scientific understanding of this part of the Mars planetary system has progressed as a result, particularly with respect to atmospheric composition, structure and the physical processes governing atmospheric motions. However, much of the insight gained in the past decade has been with respect to either the lower (0-60 km) or the upper atmosphere of Mars, not the middle atmosphere. The middle atmosphere has been neglected by the scientific community, largely due to a lack of available data for this region.

Recently, however, a growing amount of data has been collected for this region and is being made available for study. In particular, density and temperature profiles from Mars EXpress SPectroscopy for the Investigation of the Characteristics of the Atmosphere of Mars (MEX/SPICAM) stellar occultations are recently available for analysis. Analysis of this new database offers an opportunity to improve our understanding of both the structure and the underlying physics governing the dynamics of this region and how the upper and lower atmospheres interact and affect one another through exchanges in this layer.

This investigation characterizes the mean and wave structure of the middle atmosphere using the SPICAM density dataset and its corresponding temperature dataset. Model-validation of the coupled MGCM-MTGCM at middle altitudes is also performed by comparing simulated densities and temperatures with those observed by SPICAM. Finally, the SPICAM dataset is used to constrain this coupled multi-dimensional model, facilitating exploration of the underlying physical processes controlling the structure of the middle atmosphere.

MEX/SPICAM Dataset: MEX/SPICAM Stellar occultation density and temperature profiles (~70-140 km) have been obtained from F. Forget at the Laboratoire de Météorologie Dynamique (LMD). The SPICAM instrument is a UV-IR dual spectrometer. The instrument performs stellar occultations from which atmospheric densities and temperatures are extracted [1], [2].

Model Description: The coupled NASA Ames MGCM and Michigan MTGCM framework is the principal numerical tool utilized to address the dynamical and thermal processes linking the Mars middle atmosphere with the lower and upper atmospheres and to interpret the MEX/SPICAM dataset. The MTGCM is a finite difference primitive equation model at the U. of Michigan that self-consistently solves for time-dependent neutral temperatures, neutral-ion densities, and three component neutral winds over the globe [3], [4], [5]. The MTGCM is currently driven by the NASA Ames MGCM code [6] at the 1.32 microbar level (near 60-80 km), permitting a detailed upward coupling across this boundary.

Dust Prescription: Both horizontal and vertical distribution of dust must be specified in the lower atmosphere MGCM code. Dust records from the ODYSSEY/THEMIS instrument indicate that dust loads for the aphelion season are relatively consistent from one Mars Year to the next (Fig. 1), [7]. Conversely, dust loads for the perihelion season display wide variability from one Mars Year to the next.

The SPICAM dataset was taken during Mars Year 27 (MY 27), which, inspection of the THEMIS record indicates, was a year of low dust loading near the equator. Horizontal dust distributions measured during MY 27, by THEMIS [7], are used to force the lower atmosphere in the MGCM, providing simulations that may be directly compared to the SPICAM observations. For the purpose of investigating model-sensitivity to lower-atmosphere dust loading, an additional set of simulations is created, forced with dust loads from the

MGS/TES instrument [8] (Fig. 2). For both sets of simulations, the model's response to the vertical distribution of dust is also investigated [9]. A final suite of simulations is created, employing a self-consistent interactive dust mixing scheme in which smaller, lighter particles are lofted higher into the atmosphere and remain suspended for a longer period than their larger, heavier counterparts [10].

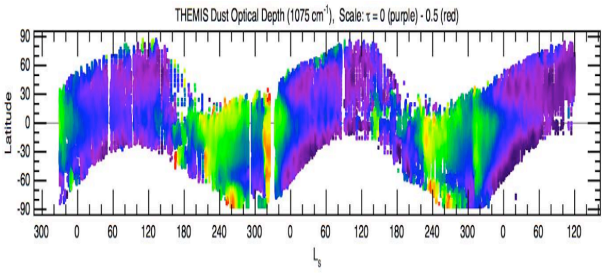

Figure 1. THEMIS dust record: Martian lower atmosphere dust opacities as a function of latitude for Ls = 330, Mars Year 25 through Ls = 120, Mars Year 28 [7].

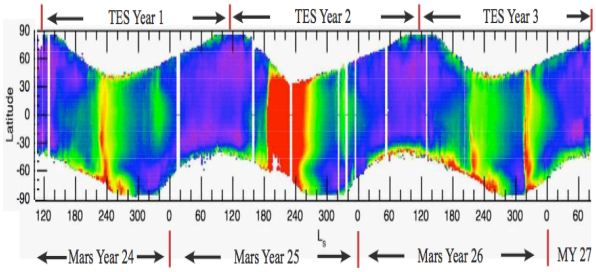

Figure 2. TES dust record: Martian lower atmosphere dust opacities as a function of latitude for Ls = 120, Mars Year 24 through Ls = 81, Mars Year 27 [9].

Methodology & Model Results: The objectives in this study are to compare the vertical structure and the seasonally-varying horizontal structure of both the density and the temperature, between observed values and the MGCM-MTGCM calculated values at middle altitudes.

To examine the vertical structure of the total density we identify the most populous 30° latitude x 2 hour local solar time (Lst) region for each of the 12 seasonal bins (Ls = 0, 30, 60, etc.) over which the calculations are performed. For each identified region, we compare the observations falling within the region to the MGCM-MTGCM simulation profile corresponding to the centroid of the region. The model captures the observed density structure in the middle atmosphere for several locations (Fig. 3). For selected locations, however, a height offset is required bring modeled densities into agreement with the observations.

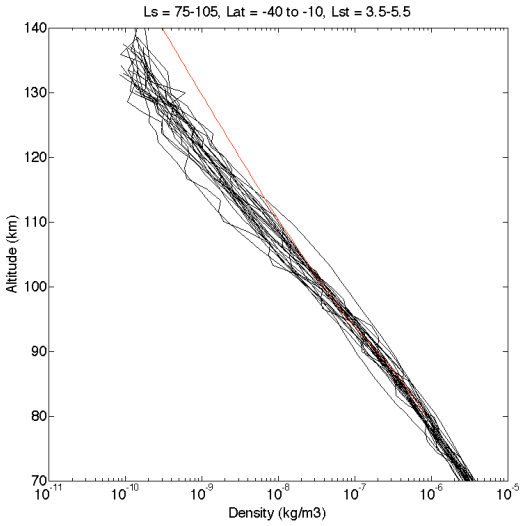

Figure 3. Observed and simulated density profiles at aphelion: black lines represents SPICAM observations falling within the specified domain; red line represents the simulation (forced with THEMIS dust loads and moderate vertical mixing depth) corresponding to the centroid of the domain. Here, while the model slightly overpredicts the densities, it captures the general vertical structure of the observed density profiles.

To explore the seasonal structure and trends of densities at middle altitudes we first obtain "best fit" simulations by creating a simulation matching the seasonal, spatial, and temporal specifications (Ls, bin, latitude, and Lst) of each individual SPICAM observation. We then compare each observation with its "best fit" simulation in a manner similar to *Forget, et al.* [11], [12] over five specified latitude ranges (90S-70S, 70S-45S, 45S-45N, 45N-70N, and 70N-90N), and at four altitude levels (80, 100, 120, and 130 km) [13], [14]. The model performs well during the low-dust aphelion season, capturing the spread of density observations and also does a reasonable job near the perihelion time period (Ls ~250-360); however it displays significant difficulty during the pre-dust-season "ramp-up" period (e.g. Ls = 120-200) (Fig. 4). Another important observation is that the model's accuracy and ability to capture the range of densities increases significantly when using appropriate dust loads (e.g. THEMIS opacities, rather than TES opacities). From this it is determined that dust loads, which affect the thermal structure of the lower atmosphere, largely influence densities in the middle atmosphere, consistent with the findings of *Bell, et al.* [9]. Hence, correct

specification of dust distribution is critical to model performance.

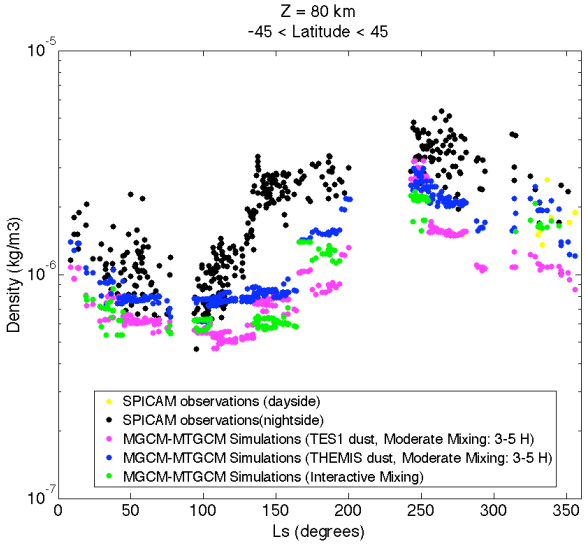

Figure 4. Seasonal density structure, at low latitudes at an altitude of 80 km. Here, the model performs well during the low-dust season (L_s = 0 – 120) and the high dust season (Ls = 250-360), but displays difficulty during the pre-dust-season "ramp-up" period (Ls = 120 – 200).

For the thermal investigation, as with the density investigation, we examine both the vertical structure and the seasonally-varying horizontal structure. Analysis and comparison of the vertical temperature structure follows a pattern similar to that used for the vertical density structure. Our method did vary slightly, however, in order to account for the tendency of temperatures to be more sensitive to local effects. To minimize the influence of local effects, rather than plotting all the observation profiles falling within the most populous region, we averaged them into one profile. In addition, to account for the wide range of longitudes represented by the observations within the most populous region, we determined that a zonally-averaged simulation profile would provide the fairest comparisons (Fig.5).

Additionally, for the purpose of facilitating comparison between different models, we compare the mean observed and calculated temperatures profile at each solstice near the equator, at the spatial and temporal specifications selected by Forget, et al. [12]. As before, in order to account for the spread of longitudes, a "best fit" simulation is calculated for each observation within the domain, at 2-hour universal time (UT) increments (i.e. 30˚ longitude increments). An average of all the "best fit" profiles is computed at each UT (longitude) increment and finally, the 12 average profiles are averaged to arrive at a zonally-averaged mean simulated temperature profile, which can be compared against the mean of the observed profiles falling within the domain (Fig. 6).

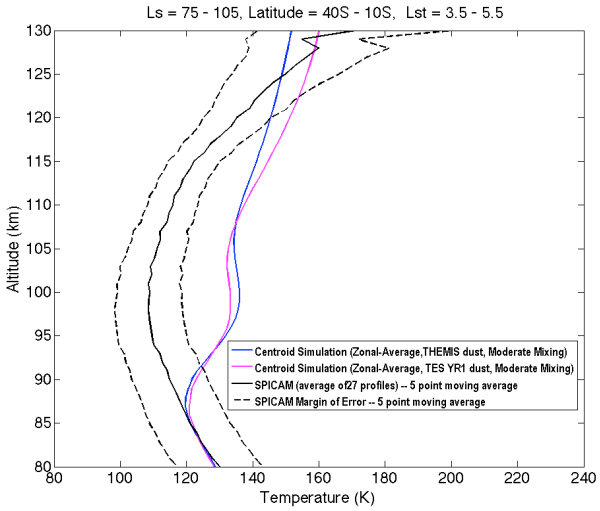

Figure 5. Observed and simulated temperature profiles at aphelion: black line represents the average of all SPICAM observations falling within the specified domain; red lines represents the margin of error in the SPICAM temperature-retrieval technique; blue line represents zonally-averaged simulation (forced with THEMIS dust loads and moderate vertical mixing depth) corresponding to the centroid of the domain. For smoothing purposes, a boxcar average is performed on the SPICAM data.

Upon discovering a discrepancy between the observed and calculated mesopause levels and temperatures, we chose to further investigate the reason for this by analyzing the vertical structure of the various heating terms that comprise the thermal balance (i.e. molecular thermal conduction, horizontal advection, adiabatic warming, total heating: EUV & IR, and IR cooling: 15 micron).

The method used to explore the seasonal structure and trends of the temperatures follows the description of the method used for the densities.

Summary: Recent datasets now make it possible to study the middle atmosphere in more detail than has occurred previously. We investigate and characterize the density and temperature structure of the Martian middle atmosphere using the SPICAM dataset. Then, we compare the observed densities and temperatures with model outputs to verify and constrain the coupled MGCM-MTGCM and uncover the physics forcing the motions of this portion of the atmosphere.

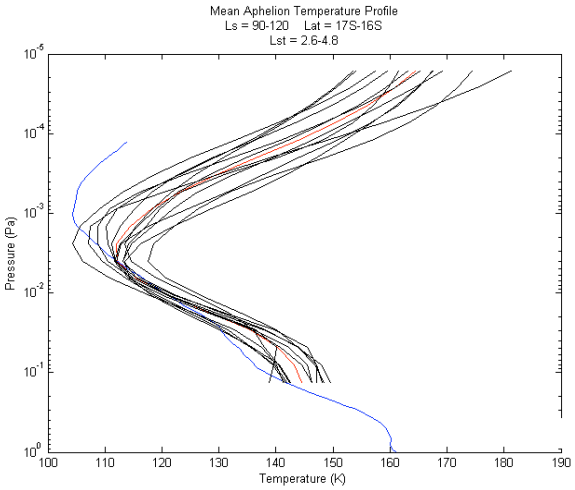

Figure 6. Mean observed and calculated temperature profiles at aphelion, between 17S and 16S latitude, and 2.6-4.8 local solar time. The blue line represents the average of the 39 SPICAM observations falling within the specified domain. The black lines represent the average of the 39 "best fit" simulations at 2-hour UT (30° longitude) increments across the globe. The red line represents the zonally-averaged mean simulated profile (average of the black profiles). The appropriate comparison is that between the red and blue profiles.

References:

[1] Bertaux, J. L. (2006) *JGR, 111,* E10S90.
[2] Quemerais, E., et al. (2006) *JGR, 111,* E9.
[3] Bougher, S. W., et al. (1999) *JGR, 104,* E7.
[4] Bougher, S. W., et al. (2000) *JGR, 105,* E7.
[5] Bougher, S. W, et al. (2006) *GRL, 33,* L02203.
[6] Haberle, et al. (1999) *JGR, 104,* E4.
[7] Smith, M. D. (2007) *Private Communication*.
[8] Smith, M.D. (2004) *Icarus, 167.*
[9] Bell, J.M, et al. (2007) *JGR*, *112,* E12002.
[10] Kahre, M. A., et al. (2008), *Icarus, 195.*
[11] Forget, et al. (2006) *IAA, Proceedings.*
[12] Forget, et al. (2007) *7th Mars,* Abstract #3029.
[13] McDunn, T. L., et al. (2007), *7th Mars,* Abstract #3087.
[14] McDunn, T. L., et al. (2008), *AGU Chapman Conference: SWIM,* Abstract #A-07.